Jurnal Teknologi

Full paper

ERT Visualization of Gas Dispersion Performance of Aerofoil and Radial Impellers in an Agitated Vessel

Mohd Sobri Takriff[a*], Azmi Ahmad[a], Masli Irwan Rosli[a], Sadiah Jantan[b]

[a]*Department of Chemical and Process Engineering, Universiti Kebangsaan Malaysia, 43600 Bangi, Selangor Malaysia*
[b]*Electrical and Electronic Section, MFI-UNIKL, Section 14, Jalan Teras Jernang, 43650 Bandar Baru Bangi, Selangor*

*Corresponding author: sobri@eng.ukm.my

Article history

Received :2 April 2013
Received in revised form :
5 June 2013
Accepted :25 June 2013

Graphical abstract

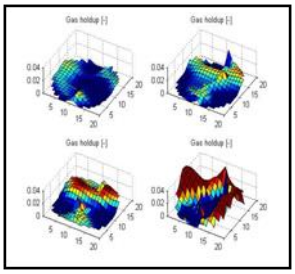

Abstract

The objective of this research work was to determine the gas dispersion performance of an aerofoil impeller and a standard Rushton turbine for gas–liquid mixing an agitated vessel via electrical resistance tomography (ERT) visualization. The experimental work was carried out in a fully baffled 400-mm-diameter agitated vessel that was fitted with four planes of 16 stainless steel electrodes connected to an ITS P2000 ERT system. Agitation was achieved by using a Lightnin Labmaster system mounted on the vessel. The ITS ERT system is equipped with a real-time data acquisition system that has the capability to capture images at up to 20 frames per second. The gas dispersion images were reconstructed using built-in image reconstruction software based on a modified linear back projection algorithm. A Matlab code was also developed to further analyse the gas dispersion by plotting a real-time surface plot from the ERT data. Various gas dispersion conditions such as flooded, transition, and dispersed were successfully visualized and characterized using the ERT technique, and over the range of the experimental works, the standard Rushton turbine was found to be a more efficient than the Lightnin A320 impeller.

Keywords: Electrical resistance tomography; gas dispersion; gas–liquid mixing; impeller flooding

1.0 INTRODUCTION

Gas–liquid mixing operations are encountered widely in the processing industries that involve physical and chemical changes. Examples of these industries are food and beverages, petroleum, chemicals, pharmaceuticals, pulp and paper, and wastewater treatment [1,2,3. Gas–liquid mixing is more complex than single phase mixing due to the dynamics of the individual phases as well as the interaction between them. An understanding of the dynamics of gas–liquid mixing is therefore crucial for optimization of designs and operation of the processing units. The best technique for determining the fundamental behaviours of a multiphase system is via visualization inside the process. Among the possible techniques for characterizing the dynamics of a gas–liquid system are computational fluid dynamics (CFD) [4], optical sensors [5], and electrical resistance tomography (ERT) [6,7,8]. In recent years, developments of the technology have led to widespread use of ERT for industrial applications [6]. The ERT technique is becoming increasingly important because of its capacity for providing potentially detailed information on the complex internal flow and multiphase behaviour of process units non-invasively and non-intrusively [6]. ERT is a simple and robust measurement technique with a wide range of applications such as analysis of gas holdup in a bubble column [9,10], mapping of particulate multiphase flow [11], two-phase pipe flow parameter measurement [12], and gas–liquid mixing in an agitated vessel [4,11,13,14,15].

ERT has been introduced and used in various investigations for visualization of the concentration profiles and characteristics of fluid dynamics in gas–liquid systems [16]. The ERT offers a unique opportunity for a non-invasive internal visualization of gas–liquid mixing in a mechanically agitated vessel [6,7]. This system is based on the use of an array of sensors that are located along the agitated vessel. Images obtained from electrical tomography show the cross-sectional spatial variation of resistivity. With proper calibration, these images depict the distribution of phase density or phase concentration in the process [7]. Among the advantages of ERT, it is useful for validating CFD models for gas–liquid mixing, its ideal electrode is inexpensive, rugged, long lasting, nontoxic, and electrically quiet, and it provides a technique for fast data acquisition of peripherally sensed resistivity which can be reconstructed to give space-wise discrimination down to 5% [6,7,8].

Most of the gas–liquid mixing operations in the processing industries are performed in mechanically agitated vessels. One of the critical factors in the design of these vessels is the selection of the impeller type. Impellers are traditionally divided into two broad categories, namely radial or axial flow impellers, depending on the main direction of the fluid motion that is induced by the rotation of the impeller. A radial impeller such as the Rushton turbine is generally accepted as a more efficient impeller for gas–liquid mixing. The aerofoil is another category of impeller that features mixed flow fluid motion due to its rotation with potential for gas–liquid operation. Thus, this paper reports the findings of ERT visualization of gas dispersion performance in a mechanically agitated vessel mounted with a radial impeller and an aerofoil impeller.

2.0 EXPERIMENTAL WORK

The experimental work was carried out in a fully baffled agitated vessel with a diameter of 400 mm and a height of 560 mm. The vessel was equipped with an ITS P2000 ERT system, where the vessel was fitted with four planes of 16 stainless steel ERT electrodes designated as P1, P2, P3, and P4 from bottom to top of the vessel. Air was fed into the vessel through several nozzle spargers located at the vessel's bottom directly below the impeller. Water was used as the continuous phase while air was used as the dispersed phase. The experimental rig was also equipped with a dissolved oxygen probe connected to a portable data logger to determine the oxygen concentration in the water with time.

The impellers used in this experiment were a 130-mm-diameter Lightnin A320 aerofoil impeller and a 133-mm-diameter radial flow Rushton turbine. The Lightnin A320 is a high flow aerofoil impeller for higher viscosity and gas applications while the standard Rushton turbine has been accepted in industry as an effective impeller for gas–liquid mixing. The diameters of the impellers used in this work were within the standard impeller diameter to vessel diameter (D/T) ratio of 1/3. The D/T ratios for the Lightnin A320 aerofoil impeller and Rushton turbine were 0.325 and 0.332, respectively. Two parameters were investigated in this experimental work, namely the type of impeller and the impeller speed. The speed range of the impeller was up to 400 rpm while the gas-flow rate was between 2 and 8 L/min.

The ITS P2000 ERT system is equipped with a real-time data acquisition system that has the capability to capture images at up to 20 frames per second. The gas dispersion images were reconstructed from the electrical conductivity data collected by the data acquisition system using built-in image reconstruction software. The software used a modified linear back projection algorithm for reconstruction of the gas dispersion images. A Matlab code was also developed to construct a real-time surface plot for gas dispersion from the ERT data. The ERT tomograms and the surface plots for various gas dispersion conditions were analysed and compared with the physical observations.

3.0 RESULTS AND DISCUSSION

The first set of experimental work was carried out to determine the imaging capability of the ITS P2000 ERT system for imaging various gas dispersion conditions. This part of the investigation study was carried out using the standard Rushton turbine. The impeller speed and the gas flow rates were adjusted to achieve the desired gas dispersion conditions. Selected tomograms from this study are presented in Figure 1 together with theoretical images for the same gas dispersion conditions [3]. The colours on the tomogram represent the mixing conditions of the fluids used in the experiment based on the values of their electrical conductivities. The red coloured region is the area with the highest value of electrical conductivity (0.15 mS/cm), which was pure water, while the dark blue coloured region represents the area with the lowest value of electrical conductivity (0.09 mS/cm), where the gas phase was concentrated. Figure 1(a) shows that there is a concentration of gas at the centre of the agitated vessel that represents the impeller flooding condition, as illustrated by the theoretical image in Figure 1(d). The ERT tomogram in Figure 1(b) shows that the gas dispersion condition improved compared to Figure 1(a); however there is a small area in the centre of the upper section of the vessel that is dominated by the gas phase, and this is similar to the theoretical transition condition, as illustrated in Figure 1(e). The ERT tomogram in Figure 1(c) shows a dispersed condition where almost all of the area within the agitated vessel was covered with gas bubbles. However this tomogram shows that the gas is not quite fully dispersed, as illustrated in Figure 1(f), since there are still some areas that are not covered by gas, as indicated by the red coloured regions. The results of this study show that ITS P2000 successfully visualized real-time images of various gas dispersion conditions inside the agitated vessel.

Table 1 Experimental parameters

Items	Specifications	
Agitated vessel	Diameter, T = 40 cm, Height, H = 56 cm, H/T = 1.4	
Baffle plates	Baffle plate width, B = 3.8 cm, B/T = 0.1	
Motor	Rotational speed = 0–550 rpm	
Impellers	Rushton turbine D_i = 13.4 cm, N_p = 6	
	Lightnin A320 D_i = 12.7 cm, N_p = 0.64	
Sparger	Five nozzles D_n = 3.0 mm	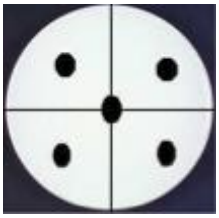

Further experiments were then carried out to determine the dispersion performance of the standard Rushton turbine and the Lightnin A320 aerofoil impeller. Table 2 summarizes the experimental data including physical observations made during each experimental run at a gas flow rate of 8 L/min. The surface plots of the gas dispersion conditions plotted using the developed Matlab code are also presented in this table. The surface plots of

each set of experimental data are for individual planes of ERT electrodes, where, starting from the top left corner, the plots represent P1, P2, P3, and P4 in the clockwise direction. The surface plots for the standard Rushton turbine show that the impeller was flooded. This is consistent with the visual observations that were made. The areas represented by the dark blue region covered some sections of the vessel, indicating that the gas phase was concentrated in certain area, while regions coloured dark red indicate that no gas phase was present. The gas dispersion situation was worst for the Lightnin A320 aerofoil impeller. The gas was not dispersed well and only concentrated randomly around the impeller region. From visual observation it was found that the gas phase was highly concentrated around plane 3 to plane 4, which implied that the impeller was flooded. In addition, the gas phase was concentrated in the upper section of the vessel, indicating that little gas was dispersed in the lower section of the vessel

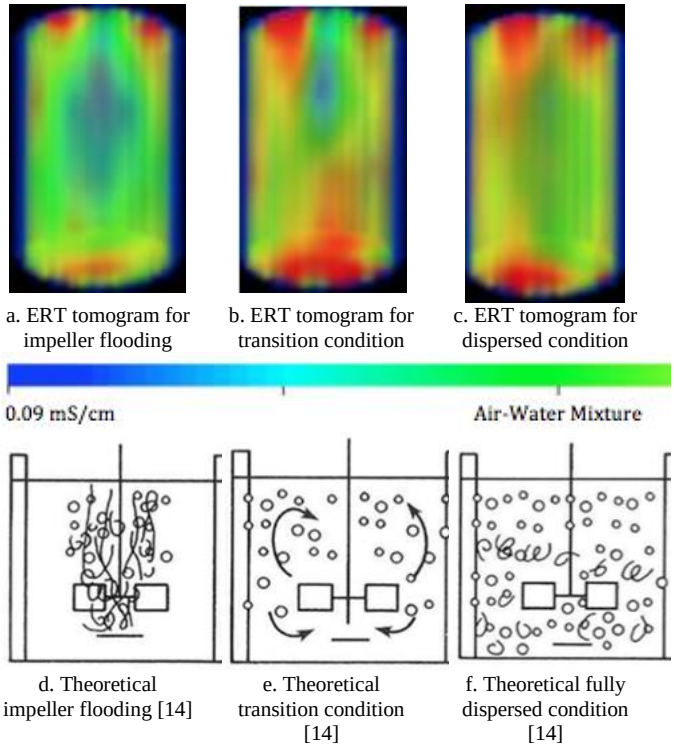

a. ERT tomogram for impeller flooding | b. ERT tomogram for transition condition | c. ERT tomogram for dispersed condition

d. Theoretical impeller flooding [14] | e. Theoretical transition condition [14] | f. Theoretical fully dispersed condition [14]

Figure 1 Various gas dispersion conditions

A summary of the experimental results at 400 rpm with a gas flow rate of 8 L/min is presented in Table 3. The surface plots presented in Table 3 for both impellers show that as the speed of the impeller increased to 400 rpm, completely different gas dispersion patterns can be clearly observed. For the standard Rushton turbine, the surface plots showed that the gas was quite well dispersed and spread radially and axially, covering the liquid region. This was confirmed by visual observation. There were, however, areas that were not covered by the gas phase. Such an observation implied that the gas was in dispersed condition but yet to reach the fully dispersed condition. The gas dispersion condition for the Lightnin A320 aerofoil impeller at 400 rpm was visually observed to be better than at 200 rpm, as discussed earlier. The impeller was not flooded; however the dispersion of the gas phase was only limited to certain regions of the vessel, as illustrated by the surface plots. These plots indicate that some regions were not covered by the gas phase, as illustrated by the dark red colour. This gas dispersion condition reflected a transition dispersion condition, as illustrated in Figure 1(e).

Table 2 Summary of experimental results at 200 rpm

Impeller	Impeller speed	Visual observation	Gas dispersion surface plot
Rushton	200 rpm	Flooded	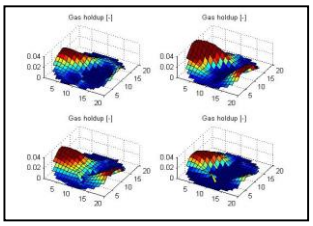
Lightnin A320	200 rpm	Flooded	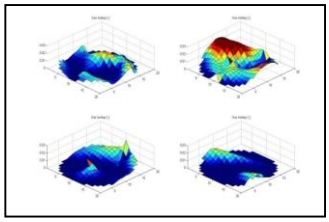

Table 3 Summary of experimental results at 200 rpm

Impeller	Impeller speed	Visual observation	Gas dispersion surface plot
Rushton	400 rpm	Dispersed	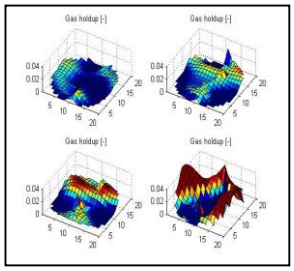
Lightnin A320	400 rpm	Loaded	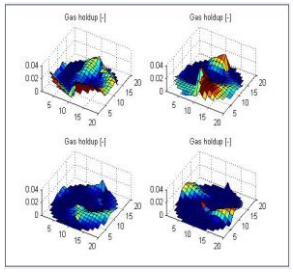

To further determine the performance of the standard Rushton turbine and the Lightnin A320 aerofoil impeller, the mass transfer coefficients for the two impellers at various speeds were plotted in Figure 2. This figure shows that at 100 rpm, where both impellers were flooded, the mass transfer coefficients had approximately the same value. However, as the impeller speeds were further increased, the value of the mass transfer coefficient for the standard Rushton turbine was much higher compared to that of the Lightnin A320 aerofoil impeller. Higher values of the mass transfer coefficient implied a better gas dispersion performance of the impeller.

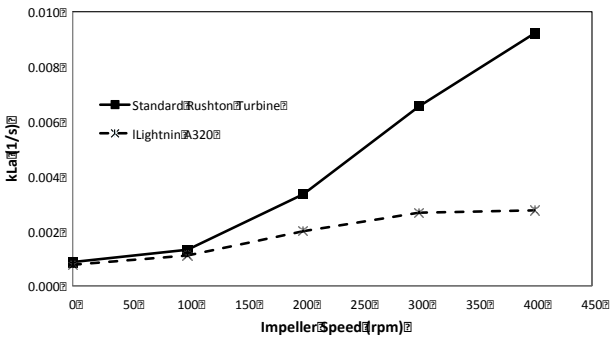

Figure 2 Mass transfer coefficient as a function of impeller speed

The results of the ERT visualization as well as the mass transfer coefficients showed that the standard Rushton turbine is a more efficient impeller for gas–liquid mixing. It is able to disperse the gas to almost all of the liquid area, leading to better mass transfer between the phases. These attributes are the desired features in the processing industry. This conclusion could be misleading, however, as it was entirely based on the comparison of the impellers' speeds. Table 1 shows that the impeller power number (N_P) of the standard Rushton turbine is more than nine times higher than that of the Lightnin A320 aerofoil impeller. For the same impeller size and at the same impeller speed, the standard Rushton turbine would require nine times more power. Even though the standard Rushton turbine is able to provide better gas dispersion and higher mass transfer, it is at the expense of higher power cost. The maximum limit of the impeller speed of the experimental rig prevents further experiments using the Lightnin A320 aerofoil impeller at higher speeds for additional investigation of the performance of this impeller. Further inspection of Figure 2 should provide some insight into the possible effects of increasing the speeds of the Lightnin A320 aerofoil impeller on its gas–liquid mixing performance. Based on the data trend shown on this figure, a further increase of the impeller speed by a few times to match the power requirements of the standard Rushton turbine may not be able to provide the same level of mass transfer coefficient, as the impeller may reach the limits of its gas dispersion. Considering the overall aspects of gas dispersion in the agitated vessel, the use of the standard Rushton turbine is more advantageous compared to the Lightnin A320 aerofoil impeller.

4.0 CONCLUSIONS

Various real time gas dispersion conditions were successfully visualized using an ERT system, and the ERT tomograms matched those of the theoretical gas dispersion conditions in an agitated vessel. The non-invasive and non-intrusive ERT imaging system can be used to compare the performances of various potential impellers in the process of selecting the optimum impeller gas–liquid processing units. The real-time images of the interaction between the gas and liquid phases in the vessel provide an insight into the fluid dynamics within the processing units. Therefore, the ERT can be used as a tool for impeller selection and to determine the optimum operating conditions for gas–liquid mixing in an agitated vessel.

The ERT imaging carried out for gas–liquid mixing in an agitated vessel also showed that the standard Rushton turbine is a more efficient impeller than the Lightnin A320 aerofoil impeller despite having a higher power requirement. This is supported by the ERT tomograms, which showed that a better gas dispersion can be achieved using the standard Rushton turbine. In addition the mass transfer coefficient data trend also supported this conclusion.

Acknowledgements

The authors thank the Ministry of Higher Education for funding this project under grant number ERGS/1/2012/TK05/UKM/01/1.

References

[1] Oldshue, J. Y. 1983. *Fluid Mixing Technology*. New York: McGraw-Hill.
[2] Paui, E. L., Atieomo-Obeng, V. A. & Kresta, S. M. 2004. *Handbook of Industrial Mixing Science and Practice*. Wiley.
[3] Tatterson, G. B. 1991. *Fluid Mixing and Gas Dispersion in Agitated Tanks*. New York: McGraw-Hill.
[4] Vesselinov, H. H., Stephan, B., Uwe, H., Holger, K., Günther, H & Wilfried, S. 2008. A Study on the Two-phase Flow in a Stirred Tank Reactor Agitated by a Gas-Inducing Turbine. *Chemical Engineering Research and Design.* 86: 75–81.
[5] Córdova-Aguilar, M. S., Díaz-Uribe, R., Escobar, O., Corkidi, G. & Galindo, G. 2008. An Optical Approach for Identifying the Nature and the Relative 3D Spatial Position of Components of Complex Structures Formed in Multiphase Dispersion Systems. *Chemical Engineering Science*. 63: 3047–3056.
[6] Dyakowski, T. 2005. Application of electrical capacitance tomography for imaging of industrial processes. *Journal of Zheijing University Science*. 6A(12): 1374–1378.
[7] Mann, R. 2005. Electrical Process Tomography: Seeing Without Eyes Inside Stirred Vessels. *Journal of Zhejiang University Science.* 6(A): 1379–1385.
[8] Wang, M., Dorward, A., Vlaev, D. & Mann, R. 2000. Measurements of Gas–Liquid Mixing in a Stirred Vessel Using Electrical Resistance Tomography (ERT). *Chemical Engineering Journal*. 77: 93–98.
[9] Fransolet, E., Crine, M., Marchot, P. & Toye, D. 2005. Analysis of Gas Holdup in a Bubble Column with a Non-Newtonian Fluid Using Electrical Resistance Tomography and Gas Dynamics Disengagement Techniques. *Chemical Engineering Science*. 60: 6118–6123.
[10] Jin, H. Wang, M. & Williams, R. A. 2007. Analysis of Bubble Behaviors in Bubble Columns Using Electrical Resistance Tomography. *Chemical Engineering Journal.* 130: 179–185.
[11] Wang, M. 2005. Impedance Mapping of Particulate Multiphase Flow. *Flow Measurement Instruments*. 18: 183–189.
[12] Dong, F., Jiang, F. Z., Qiao, X. T. & Xu, L. A. 2003. Application of Electrical Resistance Tomography To Two-Phase Pipe Flow Parameter Measurements. *Flow Measurement Instruments*. 14: 183–192.
[13] Takriff, M. S., Ahmad A. & Kamaruddin, S. K. 2010. ERT Imaging of Gas–Liquid Mixing in Agitated Vessel. *Journal of Chemistry and Chemical Engineering.* 4(29): 24–28
[14] Takriff, M. S, Hamzah, A. A., Kamaruddin, S. K. & Abdullah, J. 2009. Electrical Resistance Tomography Investigation of Gas Dispersion in Gas–Liquid Mixing In An Agitated Vessel. *Journal of Applied Sciences.* 9(17): 3110–3115.
[15] Slater, L., Binley, A., Versteeg, R., Cassiani, G., Birken, R. & Sandberg, S. 2002. A 3D ERT Study Of Solute Transport In A Large Experimental Tank. *Journal of Applied Geophysics*. 49 (4): 211–229.
[16] Holden, P. J., Wang, M., Mann, R., Dickin, F. J. & Edwards, R. B. 1999. On Detecting Pathologies Inside a Stirred Vessel Using Electrical Resistance Tomography. *Transactions of IChemE.* 77(Part A): 709–712.